AUTOMATED AIR CONDITIONING SYSTEM FOR AGRICULTURAL PRODUCT DRYING AND STORAGE

Daniel K. D. Villa[1*], Evandro de C. Melo[2], José V. Nicacio[2], Tarcísio de A. Pizziolo[2]

[1*]Corresponding author. Universidade Federal do Espírito Santo/Vitória - ES, Brasil.
E-mail daniel.villa@ufes.br | ORCID ID: https://orcid.org/0000-0002-8345-5590

KEYWORDS

control, temperature, relative humidity, air velocity, post-harvest.

ABSTRACT

This study proposes automating an air conditioning system for drying and storing agricultural products. The main objective is to precisely control key parameters of the air, namely temperature, relative humidity, and air velocity, to optimize the drying process. The framework required for constructing and operating the automated air conditioner is explained in detail. Specifically, we describe the conditioning unit, the automation hardware, the control strategies employed to regulate temperature, relative humidity, and air velocity, and discuss the safety measures and human-machine interfaces of the system. Experimental validation of the proposed system is presented, along with results and discussions demonstrating its successful control of drying air parameters across a wide range of desired conditions.

INTRODUCTION

Drying and storage are crucial post-harvest processes for seeds and medicinal plants, ensuring the preservation of their physical and chemical characteristics similar to those found in fresh plants (Lisboa et al., 2020). Temperature, relative humidity, and air velocity are key air parameters that significantly impact drying efficiency (Sivakumar et al., 2016). Traditional drying methods involve passing hot, low-humidity air through grains, allowing the air to absorb water efficiently. However, this approach has faced criticism in numerous studies (Wang et al., 2021; Silva et al., 2008). Elevated temperatures (>50°C) required to achieve low relative humidity can lead to excessive drying or overheating of grains, resulting in quality loss and increased process costs (Oliveira, 2013).

Extensive research has explored alternative approaches to high temperature drying (Bala, 2016; Onwude et al., 2016; Tiwari, 2016; Regal et al., 2020; Souza et al., 2020). However, grains are extremely sensitive to heat (Oliveira, 2013), and inadequate drying can negatively impact qualitative factors such as acidity, protein levels, germination, and appearance. On the other hand, drying at low temperatures with high relative humidity can impede the drying process, prolong drying time, and increase vulnerability to pathogens (Leprince et al., 2017).

Given the diverse drying and storage conditions specific to different plants, an automated and customizable system capable of measuring and controlling the main air parameters would greatly benefit these activities. In this context, the objective of this technical article is to propose an automated system that enables users to acquire and precisely control the temperature, relative humidity, and air velocity of the drying air within predetermined limits.

MATERIAL AND METHODS

Aminco air conditioning unit

To construct an air conditioner capable of controlling temperature, relative humidity, and air velocity, several components are required, including a humidifier, a refrigeration unit, a heater unit, sensors to measure the parameters of the drying air, and a logical unit (such as a microcontroller) responsible for process control. In this work, we propose the automation of the Aminco-Aire air conditioner, manufactured by Aminco, as the foundation for our system. Originally, this equipment allowed for closed-loop control of air temperature, requiring manual adjustment of the desired temperature. The manipulation of relative humidity was also possible but only manually and in an open-loop manner. To accommodate our automation

approach, we retained the necessary actuators from the Aminco-Aire unit while replacing the original control boards and sensors.

The Aminco conditioner can be divided into two main compartments: an upper compartment and a lower compartment, as illustrated in Figure 1. The upper compartment is further divided into three chambers, as shown in Figure 2: one for air inlet (15 cm x 75 cm), one for water spraying and air saturation (45 cm x 75 cm), and one for temperature control and air outlet (60 cm x 25 cm). The air inlet and outlet are facilitated through a circular passage with a diameter of 15 cm. In the lower compartment, a refrigeration unit (0.75 kW) and a water pump (0.18 kW) are installed to drive water to the humidifier spray nozzles.

FIGURE 1. Overview of the Aminco-Aire conditioner compartments.
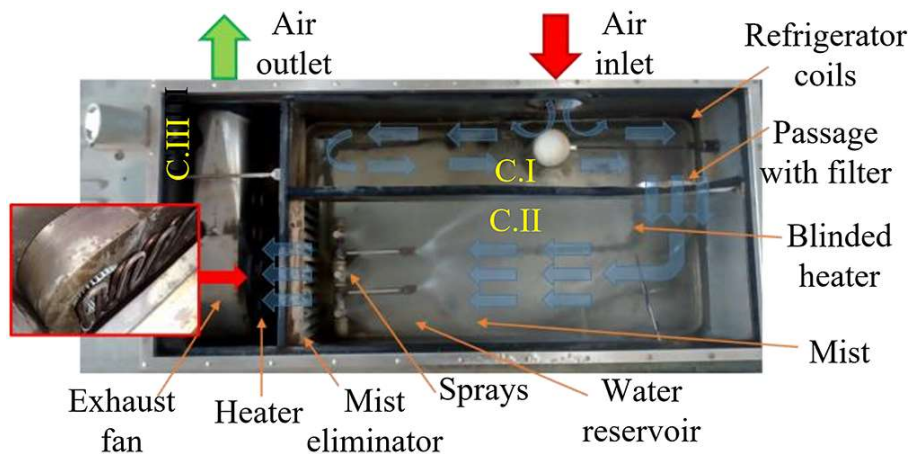
FIGURE 2. Conditioning chambers I, II, and III, serving the purposes of air inlet, spray, and air outlet, respectively (Fortes et al., 2006).

The upper compartment of the Aminco conditioner features three chambers separated by aluminum walls. A circular passage with a filter, measuring 15 cm in diameter, allows air to flow between Chamber I and Chamber II. Both chambers I and II house a shielded heater (3 kW) and the refrigeration coil, which are submerged in a water reservoir that fills the bottom of these chambers. The water level in the reservoir ensures that air can only pass between chambers I and II through the filtered circular passage and not through any other means.

Within Chamber II, there are five spray nozzles, and to proceed to Chamber III, the air must pass through a mist eliminator. The water sprayed by the nozzles is sourced from the water reservoir and its temperature is regulated by the shielded heater and refrigeration coil. Chamber III is equipped with two heaters (totaling 3 kW) responsible for heating the air. An exhaust fan propels the air towards the outlet passage, making it ready for use in drying or storage purposes.

Automation hardware

To control drying air temperature, relative humidity, and air velocity, sensors were installed in the air outlet of the conditioner, allowing closed-loop feedback control to achieve the desired conditions.

The air temperature and relative humidity sensor used was the SB-56 from Full Gauge Controls, which underwent calibration using the Hobo data logger U14-001. For air velocity measurement, a vane anemometer was implemented, constructed from a commercial microprocessor cooler measuring 9.5 cm x 9.5 cm. The cooler's tachometer employs Hall sensors, allowing for straightforward adaptation to measure air velocity. The DC motor of the cooler was removed since it is the drying air that must rotate the fan blades. With each rotation of the blades, the hall sensor generates a voltage pulse that is transmitted to the logic control unit. A counter block was employed within the control unit to count the revolutions per minute (RPM). To calibrate the relationship between blade rotation and air velocity, an FMA-900 hot-wire anemometer from Omega was employed. Figures 3A and 3B depict the arrangement of sensors in the outlet passage of the conditioner, while Figure 3C displays the calibration curve.
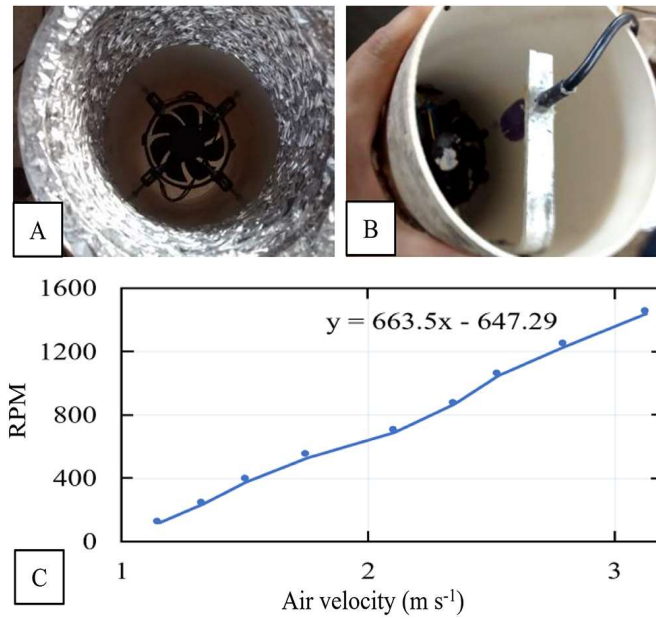
FIGURE 3. Frontal view of the vane anemometer built (A). Temperature and relative humidity sensor (B). Relationship between rotation of the cooler and velocity of the exhaust air (C).

A Full Gauge Controls SB-19 temperature sensor was installed to measure the water temperature in chambers I and II's reservoir. This measurement was crucial to ensure the water temperature remained within safe operational limits, preventing freezing, or boiling.

For system automation and control, a WEG CLIC-02-20VTD programmable logic controller (PLC) was employed as the logic unit. Five loads required control: the water pump, refrigeration unit, submerged shielded heater, outlet chamber heater, and exhaust fan. Except for the exhaust fan, the sensors and loads were connected to the respective input and output terminals of the PLC. The fan, on the other hand, was connected to a Delta 15L23A variable-frequency drive (VFD), enabling its frequency to be controlled via the Modbus protocol by the PLC.

The response curves of the sensors are presented in eqs (1), (2), and (3), which describe the relationship between the input signal and their corresponding measurements. These equations were implemented in the PLC to obtain the necessary feedback for the PID control.

$$T(°C) = 86.58 - 22.12 \times voltage(V) \qquad (1)$$

$$RH\% = (voltage(V) - 0.808) * 30.37 \qquad (2)$$

$$Airvel(ms^{-1}) = 0.98 + 0.0015 \times RPM \qquad (3)$$

The mathematical models for the SB-56 sensor, described by eqs (1) and (2), were provided by the manufacturer. Meanwhile, the model for the anemometer, given by [eq. (3)], was obtained through linear regression analysis, as depicted in Figure 3C.

Control

The operational principle adopted to control temperature and humidity is as follows. During operation, the exhaust fan and the water pump are always turned on, causing the air to flow as depicted in Figure 2. Consequently, the air passes through the mist region generated by the sprays in chamber II, achieving saturation.

By regulating the temperature of the sprayed water, the air reaches chamber III at a controlled dew point temperature, enabling control over the humidity ratio (or mixing ratio) of the drying air. Manipulating the humidity ratio allows for control of the relative humidity at the desired drying air temperature. Specifically, for a controlled temperature of the air exhausted from the conditioner, heating or cooling the water sprayed in chamber II will respectively increase or reduce the relative humidity of the drying air. Temperature control is conducted in chamber III, ensuring that the drying air delivered by the air conditioner achieves the desired temperature and relative humidity.

The drying air heater in chamber III is activated by PWM switching using a solid-state relay, controlled by a PID loop implemented in the PLC. Furthermore, due to the high transport delay in temperature response, an overdamped PID controller was adopted, which does not pose a drawback to the system considering the lengthy nature of drying and storage processes. The submerged heater and the refrigerator, responsible for heating and cooling the sprayed water, are controlled using on-off control with hysteresis.

To control the air velocity, a variable-frequency drive was used to manipulate the working frequency delivered to the exhaust fan. A PID controller adjusts the VFD frequency by comparing the signal from the air velocity sensor with the respective setpoint value. The control signal is sent to the VFD via a Modbus network. Since the air velocity varies almost instantly, it is controlled by an underdamped PID. Each of the control loops is detailed in Figure 4. The process flowchart for the automated air conditioner is presented in Figure 5.

Regarding the control loops, it is important to note that the drying parameters were controlled by decoupled loops, treating each parameter as independent. This is possible due to the time scale separation between the control loops. Specifically, the actuators can modify the air velocity much faster than the temperature, and in turn, the actuators can modify the temperature much faster than the relative humidity.

Daniel K. D. Villa, Evandro de C. Melo, José V. Nicacio, et al.

Based on the literature about drying and storage of seeds and medicinal plants, we defined the intended region of operation for the conditioner, as well as the tolerable margin of error for each of the controlled parameters. For temperature, the control range is 30 to 70 °C (± 2.5 °C). For relative humidity, the control range is 5 to 55% (± 5%). As for air velocity, the control range is 1.6 to 3.2 m/s (± 0.1 m/s).
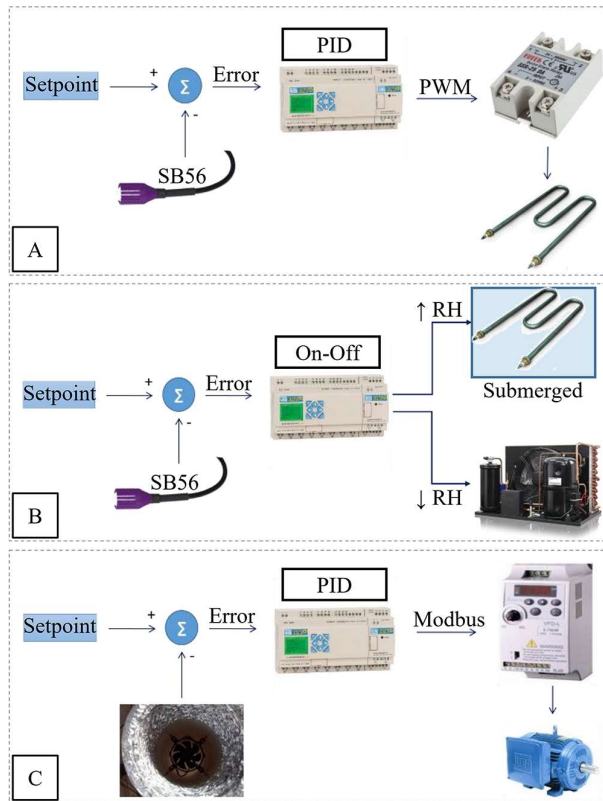
FIGURE 4. Control loops for temperature (A), relative humidity (B), and air velocity (C).
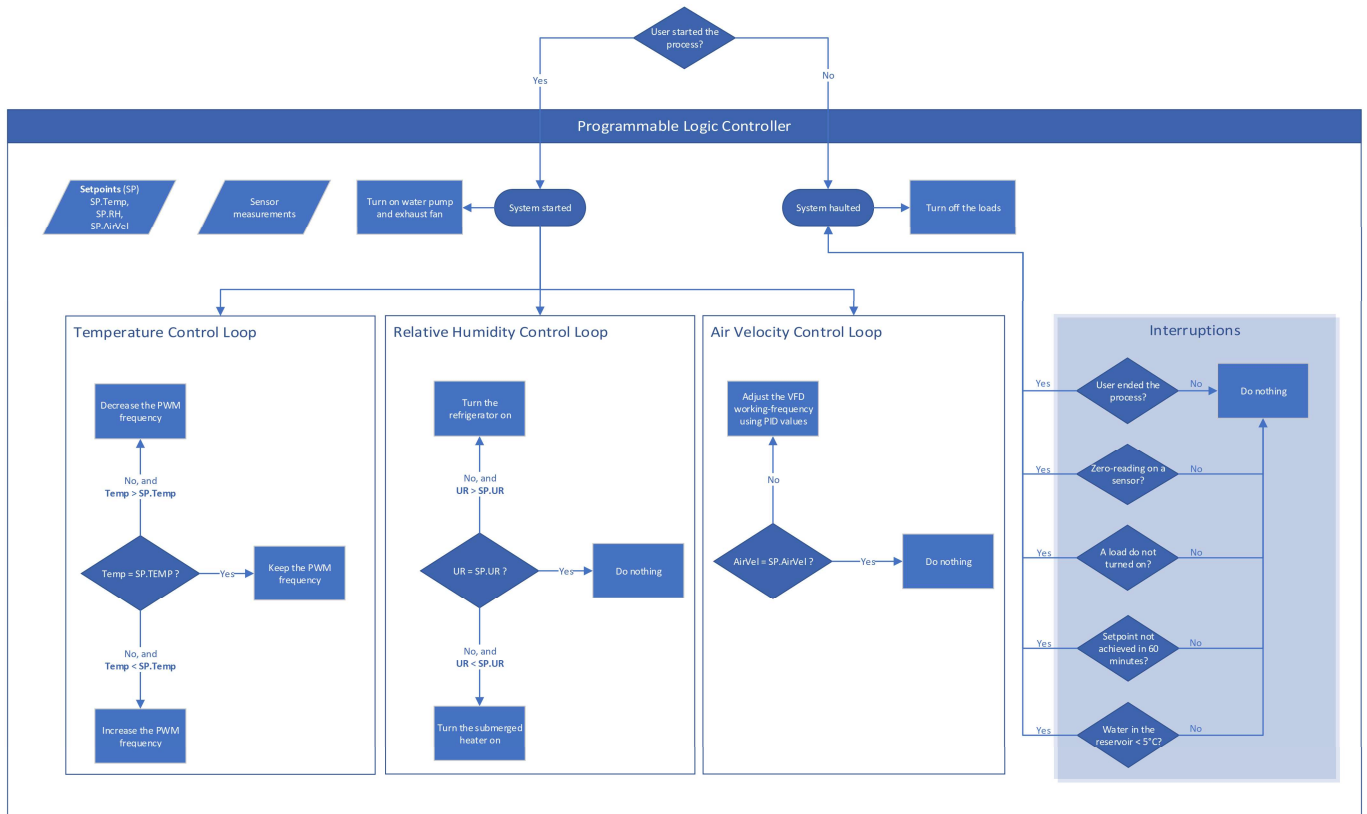
FIGURE 5. Flowchart depicting the operation of the automated air conditioner.

User interface

The PLC CLIC-02-20VTD used for automation and control incorporates a human-machine interface (HMI) consisting of four input buttons (up-arrow, down-arrow, left-arrow, and right-arrow, i.e., ↑, ↓, ←, and →) and an LCD display (4 lines x 16 characters). To facilitate user configuration and operation of the air conditioner, we developed HMI screens that enable users to initiate and terminate the automated process, monitor the current and desired values of controlled air parameters, modify the desired values, and identify the cause of any safety-related interruptions. The HMI screens can be navigated using the four input buttons.

Interface screens are categorized into configuration, operation, and alarm. The configuration screens display the current and desired states of the drying air, allowing users to initiate the drying process. These screens are presented to the user when the air conditioner is not in operation. Figure 6A and 6B illustrate the general configuration screens, which alternate on the HMI display every five seconds. Figure 6C depicts the configuration screen for the temperature setpoint, accessible by pressing the up-arrow button during the configuration screen. Screens for desired humidity and air velocity, similar to Figure 6C, are not shown. Additionally, please note that the HMI cannot display decimal values, so the read values should be divided by ten.
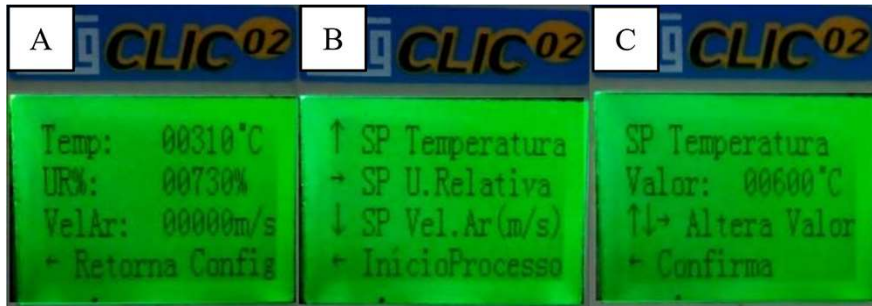
FIGURE 6. Configuration interface screens.

The operation screens are displayed once the air conditioning process has been initiated, providing users with real-time information on the current state of the drying air and the user-selected values. These interfaces also enable users to stop the process, as depicted in Figure 7A and 7B. The alarm interface screen indicates the cause of any process interruptions, alerting users to components or subsystems requiring attention or maintenance. Figure 7C illustrates a failure caused by zero readings from the air velocity sensor.

For a brief tutorial on operating the air conditioner and navigating through the HMI screens, please refer to the following link: https://youtu.be/UENXviYRVvY.
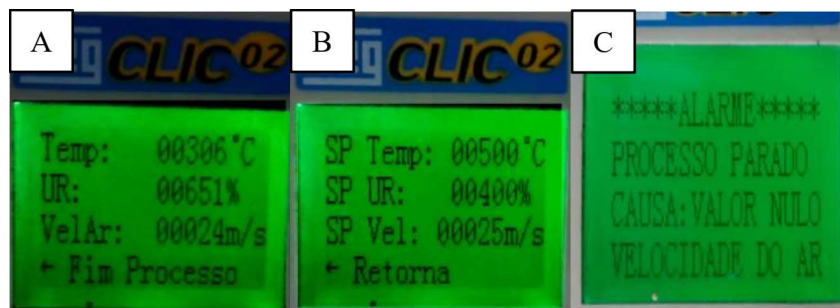
FIGURE 7. Operation interface screens (A and B). Alarm interface screen (C).

RESULTS AND DISCUSSION

This section presents the performance achieved by the automated air conditioner across various drying air setpoints. Figures 8A-C illustrate the temporal evolution of the drying air for three specific sets of desired values:

Experiment #1: Temperature 70 °C; 5% relative humidity (RH); Air velocity 2.5 m/s.

Experiment #2: Temperature 55 °C; 55% RH; Air velocity 3.2 m/s.

Experiment #3: Temperature 30 °C; 5% RH; Air velocity 1.6 m/s.

In Figures 8A-C, the blue lines represent the desired values (setpoints), while the red lines represent the actual states of the air parameters. It is crucial to note that the desired values fall within the predetermined operational limits outlined in the materials and methods section.
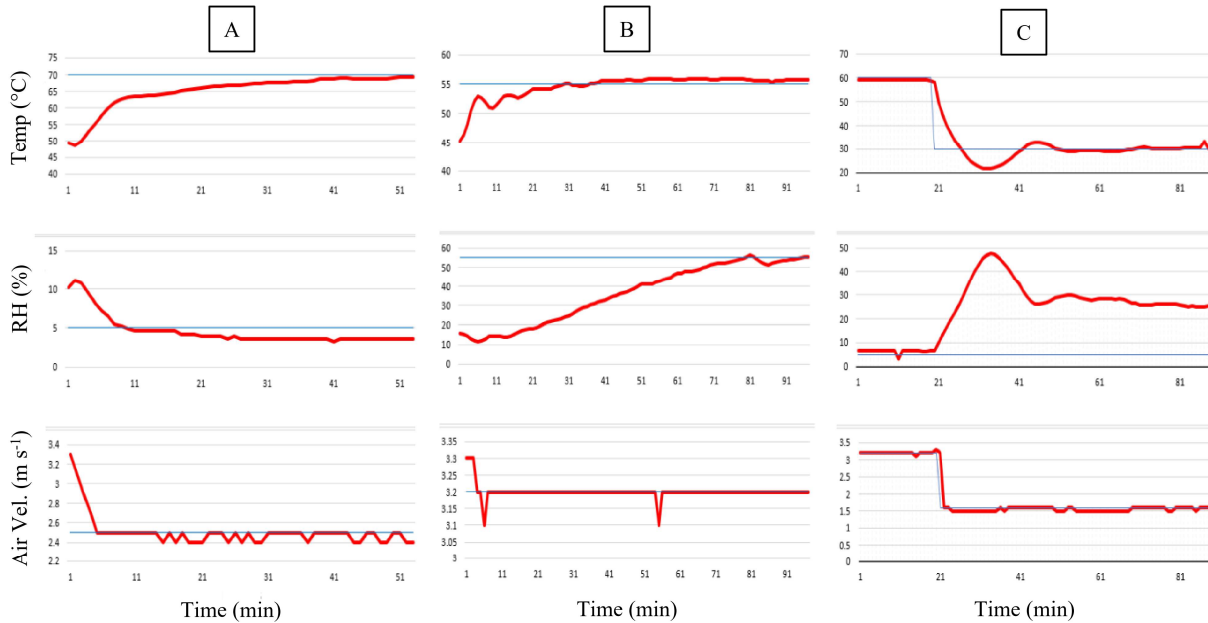
FIGURE 8. Time evolution for experiments #1 (A), #2 (B) and #3 (C).

Figures 8A and 8B demonstrate that the proposed system successfully controlled the three drying air parameters within the predefined margins for experiments #1 and #2. However, Figure 8C reveals that the system was unable to reach the desired relative humidity value for experiment #3, despite effectively controlling temperature and air velocity.

This outcome does not indicate a failure in the proposed automation and control strategies. Rather, it arises from limitations inherent to the actuators and the operation of the air conditioner, which prevent the attainment of all combinations of desired values within the established limits. As previously explained, the control of humidity ratio and relative humidity depends on the temperature of the water in chambers I and II. Using psychometric tables, it can be inferred that air at 5 °C and 100% RH has a humidity ratio of 5.42 g/kg. Since 5 °C is the minimum temperature at which the mist forms in chamber II, and since the air entering chamber III is saturated at this temperature, a humidity ratio of 5.42 g/kg represents the lowest achievable value for the proposed system.

Therefore, for a desired drying air condition of 30 °C and 5% RH, as in experiment #3, a humidity ratio of 1.31 g/kg would be required, which is unattainable in this particular system. Furthermore, Figure 8C shows that after achieving the desired temperature of 30 °C, the relative humidity reached approximately 25% in the third experiment, with the reservoir water temperature at its minimum of 5 °C. However, if the heat and mass exchange in the conditioner were perfect, saturated air at 5 °C entering chamber III would yield a relative humidity of 20.6% for a heating process up to 30 °C with a mixing ratio of 5.42 g/kg. This insufficiency in heat and mass exchange becomes even more pronounced at higher air velocities. In a trial with the same desired values as experiment #3, except for an air velocity of 3.2 m/s, the obtained relative humidity was 28%, worse than the 25% achieved at 1.6 m/s.

This analysis reveals that the heat and mass transfer in the conditioner cannot be considered flawless. Consequently, extensive experimentation was conducted to map the feasible operational regions for the automated air conditioner. Figures 9A-C illustrate these controllable regions for different air velocities. The red regions in these figures represent the predetermined control limits. As observed, the controllable area indeed decreases with increasing air velocity. It is important to note that the predefined control limits are appropriately dimensioned, as individual lower or upper limits for temperature, relative humidity, and air velocity can be achieved, as demonstrated in experiments #1, #2, and #3 and reflected in the control region figures. Furthermore, even when combining desired parameters, the proposed system can still achieve a wide range of conditions for the drying air parameters.
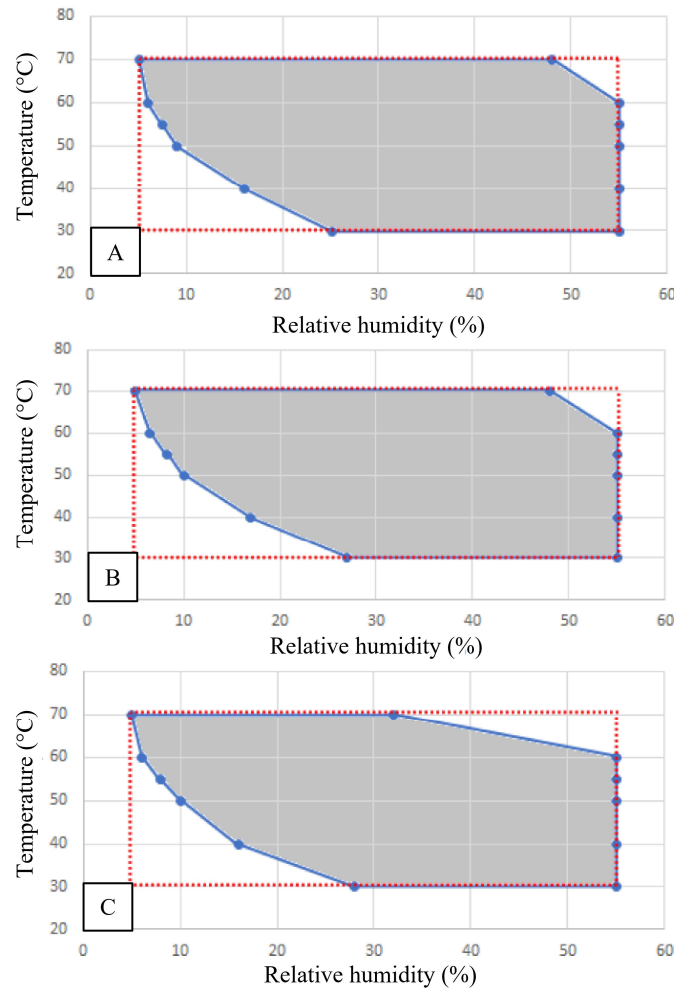
FIGURE 9. Achievable control region for air velocities of 1.6 m/s (A), 2.4 m/s (B), and 3.6 m/s (C).

The results and discussions presented above lead to the conclusion that the automated air conditioner provides users with the flexibility to independently manipulate the key parameters of the drying air. This flexibility allows for the exploration and implementation of techniques that go beyond the limitations of hot-and-dry or cold-and-humid air conditions, as evidenced by studies conducted by Santos et al. (2021), Leprince et al. (2017), Silva et al. (2022), and other researchers. Moreover, many existing drying and storage methods are susceptible to variations in external conditions, as highlighted by Lisboa et al. (2018). However, the closed system operation of this air conditioner ensures that the control of air parameters remains unaffected by fluctuations in ambient temperature or humidity. Consequently, the proposed system presents an intriguing option for precision agriculture and other related applications.

CONCLUSIONS

This work introduces the automation of an air conditioner designed for controlling the primary parameters of drying air: temperature, relative humidity, and air velocity. The conditioner offers users the ability to explore diverse drying air scenarios, enabling analysis, comparison, and advancements in drying and storage techniques for agricultural products. The article comprehensively presents the sensors, loads, hardware, and software employed for automating and controlling the conditioner, facilitating the adaptation and construction of similar systems, even for varying power requirements. Future endeavors will focus on enhancing heat and mass transfer within the system, such as optimizing the mist region in chamber II and replacing the shielded heater in chamber III with a finned heater. These modifications aim to improve heat exchange efficiency, expand the achievable control region, and ultimately expedite the system's attainment of desired setpoints across a broader range of drying parameters.

REFERENCES

Bala BK (2016) Drying and storage of cereal grains. John Wiley & Sons. https://doi.org/10.1002/9781119124207

Fortes M, Ferreira DA, Ferreira WR, Souza ACD (2006) Modelagem de um condicionador de ar de alta precisão para uso em processamento agrícola. Engenharia Agrícola 26: 578-589. https://doi.org/10.1590/S0100-69162006000200028

Leprince O, Pellizzaro A, Berriri S, Buitink J (2017) Late seed maturation: drying without dying. Journal of experimental botany 68(4): 827-841.

Lisboa CF, Melo EC, Demuner AJ, Silva LC da, Carneiro AP, Coelho APF (2020) Chemical composition of Lippia origanoides Kunt. and Ocimum gratissimum L. essential oils stored at− 20° C. Industrial Crops and Products 151: 112485. https://doi.org/10.1016/j.indcrop.2020.112485

Lisboa CF, Melo EC, Donzeles SML (2018) Influence of storage conditions on quality attributes of medicinal plants. Biomedical Journal of Scientific & Technical Research 4(4): 4093-4095.

Oliveira JB (2013) Smooth adaptive robust temperature control of a seed drying system. IFAC Proceedings Volumes 46(18): 6-11. https://doi.org/10.3182/20130828-2-SF-3019.00012

Onwude DI, Hashim N, Janius RB, Nawi NM, Abdan K (2016) Modeling the thin-layer drying of fruits and vegetables: A review. Comprehensive reviews in food science and food safety 15(3): 599-618.

Regal AL, Alves V, Gomes R, Matos J, Bandarra NM, Afonso C, Cardoso C (2020) Drying process, storage conditions, and time alter the biochemical composition and bioactivity of the anti-greenhouse seaweed Asparagopsis taxiformis. European Food Research and Technology 246(4): 781-793.

Santos IS, Nascimento BL, Marino RH, Sussuchi EM, Matos MP, Griza S (2021) Influence of drying heat treatments on the mechanical behavior and physico-chemical properties of mycelial biocomposite. Composites Part B: Engineering 217: 108870.

Silva GN, Saraiva-Grossi JA, Carvalho MS, Faroni LRDA, Lopes OP, Oliveira MS, Barbosa DRS, Silva YNM (2022) Macauba fruits preserved by combining drying and ozonation methods for biodiesel production. Ozone: Science & Engineering: 1-9.

Silva JS, Lacerda Filho SAF de, Ruffato S, Berbert PA (2008) Secagem e armazenagem de produtos agrícolas. Viçosa, MG, UFV.

Sivakumar R, Saravanan R, Perumal AE, Iniyan S (2016) Fluidized bed drying of some agro products–A review. Renewable and Sustainable Energy Reviews 61: 280-301. https://doi.org/10.1016/j.rser.2016.04.014

Souza RAD, Melo EDC, Ávila MB de, Gonzaga DA, Sperotto NC, Carneiro AP (2020) Intermittent drying of clove basil leaves: process optimization and essential oil yield. Revista Brasileira de Engenharia Agrícola e Ambiental 24: 209-215.

Tiwari A (2016) A review on solar drying of agricultural produce. Journal of Food Processing and Technology 7(9): 1-12.

Wang F, Shao W, Yang D (2021) Effect of different drying methods on drying characteristics and quality of Camellia oleifera seeds. Journal of Food Processing and Preservation 45(12): e15976.